J Appl Electrochem (2009) 39:2173–2179
DOI 10.1007/s10800-009-9841-2

ORIGINAL PAPER

Investigation of low cost carbonaceous materials for application as counter electrode in dye-sensitized solar cells

T. Denaro · V. Baglio · M. Girolamo · V. Antonucci · A. S. Arico' · F. Matteucci · R. Ornelas

Received: 29 September 2008 / Accepted: 13 February 2009 / Published online: 5 March 2009

Abstract The structural and morphologic properties of different carbonaceous materials were studied by X-ray diffraction (XRD), Brunauer–Emmet–Teller (BET) porosimetry and transmission electron microscopy (TEM) analyses. The electrochemical behaviour of these powders used as counter electrode in dye-sensitized solar cells (DSSCs) was investigated by polarization experiments and electron impedance spectroscopy. Results were compared with DSSC using Pt as counter electrode. All DSSCs based on the carbonaceous materials showed conversion efficiencies higher than those equipped with Pt. Among the various carbon materials investigated, Acetylene Black in conjunction with graphite showed the best performance. This was interpreted from the physico-chemical analysis as due to a compromise between pores accessibility for the I_3^- reactant presents in electrolyte and appropriate surface graphiticity index of this carbonaceous material. A high degree of graphitization for the carbon black was found to enhance electron conduction and charge transfer properties.

Keywords Dye-sensitized solar cells · Carbon blacks · Counter electrode · Pores accessibility · Graphiticity index

T. Denaro · V. Baglio (✉) · M. Girolamo · V. Antonucci · A. S. Arico'
CNR-ITAE Institute, via Salita S. Lucia sopra Contesse, 5, 98126 Messina, Italy
e-mail: baglio@itae.cnr.it

F. Matteucci · R. Ornelas
TRE Tozzi Renewable Energy S.p.A., via Zuccherificio, 10, 48010 Mezzano, RA, Italy

1 Introduction

Dye-sensitized solar cells (DSSCs) are well known as potentially low-cost photovoltaic devices [1]; from this perspective, the use of low-cost materials in this device is quite important. The counter electrode is one of the active components in DSSCs. The task of the counter electrode (CE) is the reduction of the redox species used as a mediator in regenerating the sensitizer after electron injection into the photo-anode. The standard catalyst in the CE in most of the recent publications in this field is platinum [1–7] because of the high catalytic activity and high corrosion stability against iodine in the electrolyte. As a precious metal, Pt is subject to price variations [8]. It is nevertheless desirable to develop alternative low-cost materials for CEs, which should be corrosion resistant and exhibit good catalytic activity for the reduction of the triiodide ion.

Carbonaceous materials are quite attractive to replace platinum due to their high electronic conductivity, corrosion resistance towards I_2, high reactivity for triiodide reduction and low cost [9–19]. The lower catalytic activity of carbon compared to platinum can be compensated by increasing the active surface area of the electrode by using a porous electrode structure. Porous carbon electrodes are easily prepared from graphite powder, which consists of platelike crystals that, on deposition from a liquid dispersion and drying, will preferentially align in the plane of the counter electrodes, resulting in a high conductivity in this plane [9, 20].

The catalytic activity of the graphite counter electrodes for triiodide reduction as well as their conductivity may be considerably enhanced by adding about 20% by weight of carbon black [21] to the dispersion of graphite powder. For good cohesion between the graphite particles and carbon

black a binder is required. This binder should withstand firing at 450 °C in air. A binder that is well compatible with the other components of the dye sensitized solar cell and adheres well to carbon is TiO_2, already used as semiconductor at the photo-anode. Counter electrodes prepared by spray coating of an aqueous dispersion of graphite powder, 20% by weight of high surface area carbon black and 15% nanocristalline TiO_2, with a particle size below 20 nm, are well adherent and scratch resistant after firing in air at 450 °C for 10 min [9].

In this work, physico-chemical properties of different carbonaceous materials used as counter electrodes were investigated by X-ray diffraction (XRD), Brunauer–Emmet–Teller (BET) and transmission electron microscopy (TEM) analyses; the electrochemical behaviour was investigated by current–voltage (I–V) and electrochemical impedance spectroscopy measurements. The results were compared with conventional Pt counter electrodes.

2 Experimental

X-ray diffraction analysis (XRD) of the carbon powders was carried out with a Philips X'Pert diffractometer equipped with a CuKα X-ray source. TEM analysis of the carbon powders was carried out with a Philips CM12 microscope. Surface area, pore size distribution and pore volume characteristics for the different carbonaceous materials, pure powders (Table 1) and mixtures (Table 2), were measured by a Thermoquest analyzer. Pore specific volume was calculated by using the B.E.T. equation (C = 12.3839); whereas, cumulative pore volume was determined by using the B.J.H. equation (C = 0.8).

Working electrodes and counter electrodes were prepared on F-doped SnO_2 glass (sheet resistance: 15Ω/□) substrates (FTO). The TiO_2 paste for the photo-anode was prepared from commercial powder (Degussa P25) and deposited by a spray technique onto the substrate. Afterwards, electrodes were sintered at 450 °C for 30 min; the sintering process allows the titanium dioxide nanocrystals to melt partially together, in order to ensure electrical contact and mechanical adhesion on the glass. Dye sensitization was carried out by immersing the sintered electrodes in 0.2 mM N_3 solution (Solaronix) in ethanol for about 16 h. Electrolyte consisted of 0.4 M LiI, 0.04 M I_2, 0.3 M 4-tertbutylpyridine (TBP) and 0.4 M tetrabutylammonium iodide (TBAI) in Acetonitrile. The Platinum counter electrode was prepared by depositing the hexachloro platinic acid based solution on FTO/glass substrate, followed by sintering at 450 °C for 30 min. Carbon powders were prepared by mixing different carbonaceous materials: high surface area (SA) graphite (Timerex Special Graphite; SA from BET: 280 m^2/g) and 20% w/w carbon black.

Table 1 Surface area and interlayer distance of the carbonaceous materials

Carbon	Surface area (m^2/g)	Interlayer distance (nm)
Graphite	280	0.33
Acetylene Black	60	0.35
Vulcan XC-72R	250	0.37
Ketjen Black	950	0.37

Table 2 Surface area and pore volume of the different mixtures of carbonaceous materials after thermal treatment

Mixture containing	Surface area (m^2/g)	Pore volume (g/cm^3)
Acetylene Black	111.4	0.25
Vulcan XC-72R	184.2	0.39
Ketjen Black	297.3	0.49

Three commercial carbon blacks with different surface areas, Ketjen Black DJ-600 EC (SA from BET: 950 m^2/g), Vulcan XC-72R (SA from BET: 250 m^2/g) and Acetylene Black (Shawinigan; SA from BET: 60 m^2/g), were used. 15% w/w of TiO_2 (Degussa P25) was added as binder to the mixture. The powders were dissolved in ethanol. Counter electrodes were prepared by spraying the slurry of carbon powders onto FTO/glass substrates, then electrodes were sintered at 450 °C for 10 min.

A spacer thick 100 μm was used to allocate the electrolyte between the photo-anode and the counter electrode. Generally, the spacing between these electrodes is about 30 μm in the state-of-art DSSCs to avoid ohmic constraints. Yet, being the aim of this work addressed to compare different materials in the same conditions, we have preferred to use a suitable amount of liquid electrolyte in between the two electrodes in order to avoid short circuit effects and improve reproducibility of the cells.

Current–voltage curves of the devices were recorded under simulated AM 1.5 solar illumination (Osram, 300 W) at 25 °C. The incident light intensity was adjusted to 100 mW cm^{-2} by using a photometer (3 M Photodine Inc.). The cells operating under simulated solar illumination were connected to an Autolab Potentiostat/Galvanostat (ECOCHEMIE) equipped with a FRA. The active area of the cells was 0.25 cm^2.

EIS measurements were carried out at room temperature in the frequency range 100 mHz to 1 MHz at open circuit voltage (OCV); the amplitude of potential pulse was 0.01 V. Electrochemical parameters were derived from the *ac* impedance spectra by using a complex non-linear least square fitting procedure contained in the EQUIVCRT software [22].

3 Results and discussion

The structure, morphology and porosity of several carbonaceous materials were investigated by XRD, TEM and BET analyses.

The XRD pattern of the graphite powder is characterized by a peak at $2\theta = 26.4°$ representing (002) reflection; it is due to the ordered structure of graphite. For Vulcan and Ketjen Black powders, the XRD analysis shows an amorphous structure; whereas, for what concerns the Acetylene Black powder, the XRD pattern indicates a more ordered structure compared to the other carbon blacks (Fig. 1).

TEM images of the various carbon materials are presented in Figs. 2 and 3, at different magnifications. Disordered structures for carbon blacks, in particular for Vulcan and Ketjen Black, are observed in these figures. A disordered lattice characterized by the absence of large-range order for the graphitical basal planes is typical of the amorphous carbons. Furthermore, all carbon blacks show a porous structure with a large presence of micro pores mainly in high surface area amorphous carbons, as shown in Fig. 4.

The interlayer spacing in the graphite-like lattice of the carbon blacks allows an estimation of the graphitization degree in these materials. In general, growing disorder in the materials is reflected in increased values of the interlayer spacing. From TEM images obtained at high magnification, it is possible to measure the interlayer spacing for the different materials. For the graphite, the interlayer distance value was 0.33 nm which is the typical value for the graphite powders. For the carbonaceous materials, the interlayer spacing are larger than graphite powder: 0.35 nm for Acetylene Black and 0.37 nm both for Vulcan and Ketjen Black. These values indicate that the carbon blacks are characterized by a larger degree of disorder. Surface area and interlayer distance for each carbon material are summarized in Table 1.

Figure 5 shows the photocurrent–voltage characteristics of DSSCs using the graphite–carbon black mixtures and Pt as counter electrodes. The carbon materials in the present work show higher performance than Pt as counter electrode. This is probably due to the high surface area of carbon blacks that compensates the lower catalytic activity of these materials compared to Platinum. Furthermore, the Pt layer was treated at 450 °C for longer times than the carbon black based electrode to favour the adhesion to the substrate. This may have reduced the active surface area by effect of sintering. The electrode using graphite–Acetylene Black mixture shows the best performance in terms of conversion efficiency (η), open circuit voltage (V_{OC}) and fill factor (FF).

The conversion efficiency is defined as follows:

$$\eta(\%) = \frac{V_{OC}\, j_{SC}\, FF}{P_S}$$

where P_S stands for the power density of the incident illumination, and the fill factor is calculated by:

$$FF = \frac{V_m\, j_m}{V_{OC}\, j_{SC}}$$

where j_m and V_m are respectively current density and voltage for maximum power output. The conversion efficiencies, FF, short circuit current density (j_{SC}) and V_{OC} of the different materials are summarized in Table 3.

A good electrochemical behaviour was also recorded for the DSSC based on pure graphite as counter electrode; in

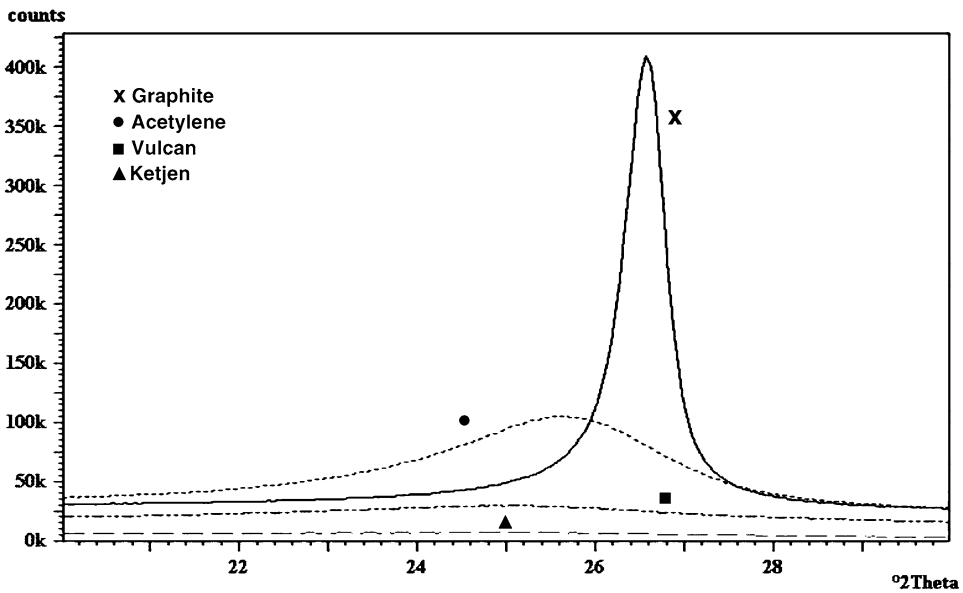

Fig. 1 XRD patterns for graphite and several carbon blacks: (—) graphite, (•••) Acetylene Black, (–•–) Vulcan XC-72R, (– –) Ketjen Black

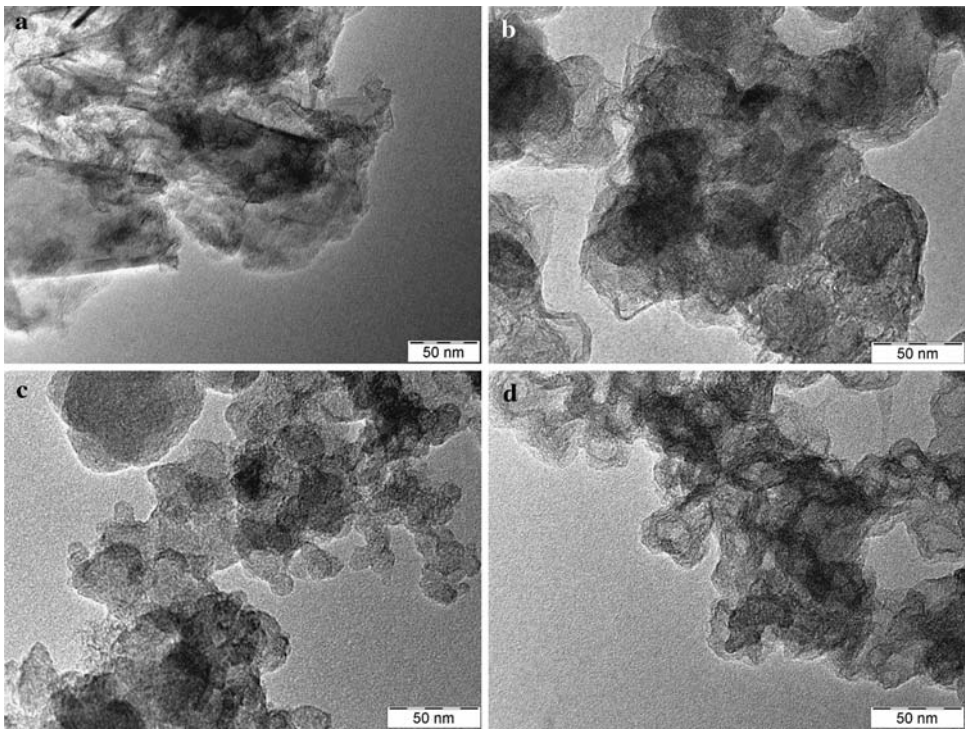

Fig. 2 TEM images of different carbon blacks: **a** Graphite, **b** Acetylene Black, **c** Vulcan XC-72R, **d** Ketjen Black

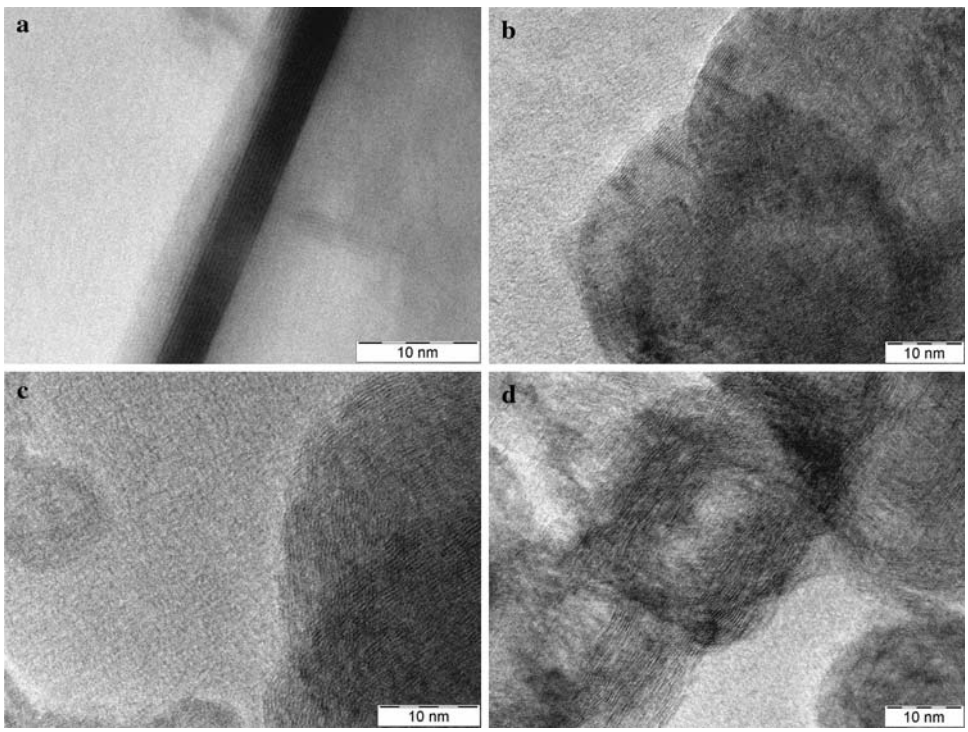

Fig. 3 High magnification TEM images of different carbon blacks: **a** Graphite, **b** Acetylene Black, **c** Vulcan XC-72R, **d** Ketjen Black. Graphite basal planes are showed in the micrographs

particular, the highest j_{SC} was observed for this cell. Also the conversion efficiency is quite promising ($\eta = 1.8\%$). By mixing the graphite powder with high surface area carbon blacks such as Vulcan and Ketjen Black, the performance decreased compared to pure graphite. This could be due to the high presence of micro pores in the carbon blacks that are not accessible for the I_3^- reactant [23]. The mixtures of graphite with Ketjen Black or Vulcan show a similar cumulative pore volume, which is about twice that observed for the mixture of graphite and Acetylene Black (Fig. 4). The presence of Acetylene Black in conjunction with graphite powder produced the best performance as a compromise between amount of available pores for the reaction and graphitic characteristics. In fact, Acetylene

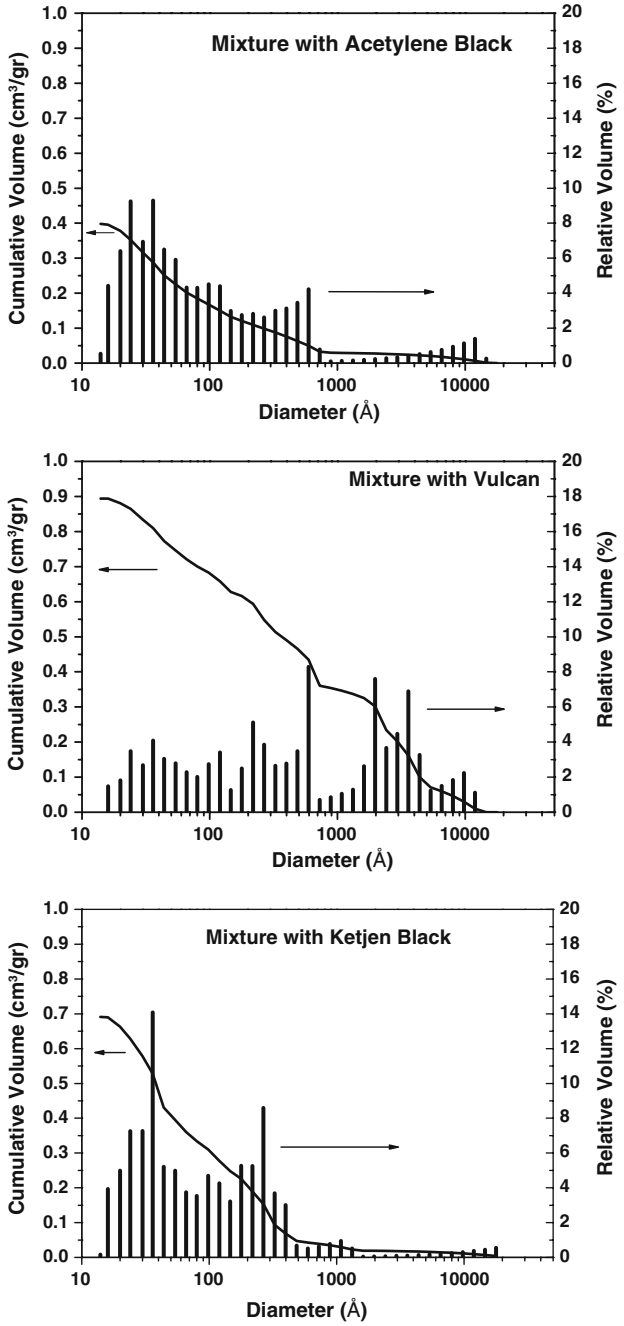

Fig. 4 Pore size distribution and cumulative pore volume in different mixtures

Black shows a higher graphitization index with respect to the other carbon blacks, which appears to reduce the charge transfer resistance of the cell (see impedance spectra in Fig. 6). Electron transfer should be favoured by a highly conjugated sp^2 electronic configuration for the carbon black based counter electrode [20]. Furthermore, this carbon black is essentially characterized by mesopores which are accessible to I_3^- ions. On the contrary, Vulcan and Ketjen Black contain mainly micro pores.

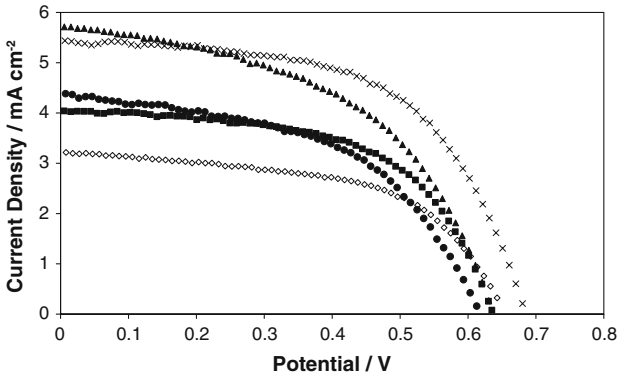

Fig. 5 I–V curves for DSSCs using different counter electrodes. (◇) Pt, (×) Graphite + Acetylene Black, (■) Graphite + Vulcan, (•) Graphite + Ketjen Black, (▲) Graphite

Table 3 Performance characteristics of DSSCs with different counter electrodes

Counter electrodes	V_{OC} (V)	j_{SC} (mA/cm^2)	*FF*	η (%)
Acetylene Black and graphite	0.69	5.43	0.57	2.15
Graphite H.A.	0.63	5.70	0.50	1.80
Vulcan and graphite	0.63	4.00	0.57	1.48
Ketjen Black and graphite	0.61	4.36	0.50	1.36
Pt	0.66	3.20	0.55	1.18

Electrochemical Impedance Spectroscopy (EIS) has been widely used to investigate the interfacial charge transfer processes occurring in DSSCs [24]. The Nyquist plots reported in the literature for DSSCs consist of two [25] or three [24] semicircles. These are generally related, in order of decreasing frequencies, to counter-electrode/electrolyte interface, TiO_2/electrolyte interface and ionic diffusion of I_3^- species in the electrolyte. Our *ac*-impedance spectra essentially show two semicircles (Fig. 6). In addition, at very low frequencies, the onset of a linear behaviour with a slope of about 45 °C is observed for all cells (Fig. 6). This is indicative of a Warburg-like diffusion component possibly related to the diffusion of ionic species

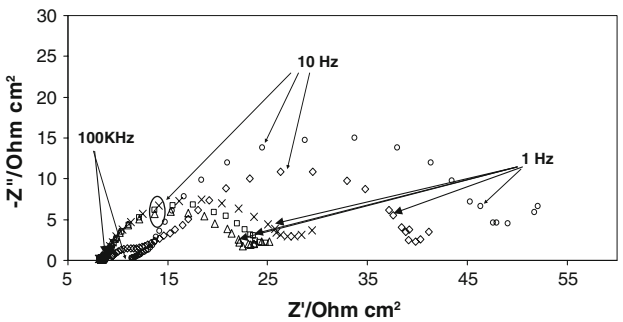

Fig. 6 Electrochemical Impedance Spectra for DSSCs using different counter electrodes. (◇) Pt, (□) Graphite + Acetylene Black, (×) Graphite + Vulcan, (○) Graphite + Ketjen Black, (Δ) Graphite

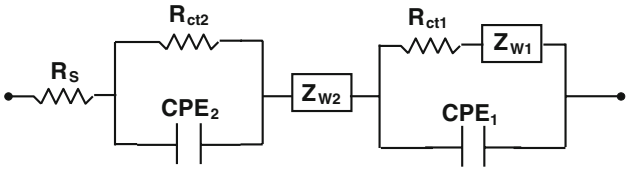

Fig. 7 Equivalent circuit of the investigated DSSCs

at the TiO_2 interface. The *ac* response due to the diffusion of ionic species in the bulk electrolyte should occur at lower frequencies. This effect is possibly not recorded in the present spectra characterized by a low-frequency limit of 0.1 Hz (a large scattering was recorded below this frequency). The main representative elements of the equivalent circuit are reported in Fig. 7. The Warburg-like diffusion element due to the transport of ionic species towards the TiO_2 pores is in series connected with the charge transfer resistance R_{ct1} at the TiO_2/electrolyte interface. This two elements being in parallel with the capacitive element (constant phase element) mainly related to the double layer capacitance originated at the porous TiO_2 electrode/electrolyte interface. Similarly, a parallel connection between the charge transfer resistance R_{ct2} and constant phase element CPE2 represents the counter electrode. The series resistance (R_S) is related to the ohmic effects (see below).

Since the performance of the counter electrode may affect also the electrochemical behaviour of the working electrode, we have considered in our analysis the total contribution to the charge transfer resistance $R_{ct} = R_{ct1} + R_{ct2}$. This was derived by the low frequency impedance by subtracting the high frequency intercept on the real axis due to Rs and the lower frequency contribution of the Warburg diffusion element. R_{ct} is, thus, the charge-transfer resistance of the electrochemical reactions at the photo-anode and the counter electrode. It is observed that the photo-anode is the same in all cells, thus the R_{ct} reflects the contribution for the counter electrode. The high frequency intercept measured under open circuit condition is related to the series resistance (R_S). It accounts for the resistance of the conductive materials in the cell with contributions from the FTO substrate layer, porous electrode material, current collector and resistivity of the electrolyte. Electrochemical impedance spectra for DSSCs using several counter electrodes are showed in Fig. 6.

R_S and R_{ct} values are summarized in Table 4. It seems that there is not a strict correlation between R_S values, which represents the ohmic contribution, and conversion efficiencies. On the contrary, conversion efficiencies are more influenced by reaction kinetics (R_{ct}). The reaction rate on the counter electrode is strictly related to the morphology and charge transfer properties of the carbon black used in the powder mixture. Thus, it is related to their surface area values, porosity, in terms of accessibility for the I_3^- reactant, and graphiticity index [20]. The latter determines the electronic conductivity in the material and influences the rate of charge transfer at the interface [26]. The cell conversion efficiencies, for the different carbon mixtures, reflect all these aspects. The carbonaceous material that shows the best compromise between electronic conductivity, as determined by the degree of graphitization, and amount of mesopores available for reduction of I_3^- ions provides the best results. It is pointed out that further optimization of the cell in terms of electrolyte thickness may enhance the conversion efficiency.

Table 4 Resistance values of DSSCs with different counter electrodes

Counter electrodes	R_S (Ohm cm^2)	R_{ct} (Ohm cm^2)
Acetylene Black and graphite	8.5	14.8
Graphite H.A.	8.5	14.0
Vulcan and graphite	7.8	16.6
Ketjen Black and graphite	11.1	38.8
Pt	9.2	30.8

4 Conclusions

Different carbonaceous materials were used as counter electrode in dye-sensitized solar cells and compared with Pt. High surface area graphite and various carbon black powders with different surface area were investigated by XRD, BET and TEM analyses. Electrochemical investigation on DSSCs were performed by I–V polarizations and EIS. Graphite–carbon black mixtures gave cell performance better than Pt due to the high surface area of carbon blacks that compensates the lower catalytic activity of these materials compared to Platinum. Accordingly carbonaceous materials appeared to be valid alternatives to noble metals as cathodes. Electrochemical impedance spectroscopy showed a correlation between the cell performance and the powder morphology, evidenced by physical-chemical characterizations. The counter electrode using graphite–Acetylene Black mixture produced the best performance, showing a good compromise between amount of available pores and graphitic characteristics.

Acknowledgement Authors acknowledge Daunia Solar Cell for financial support.

References

1. Gratzel M (2004) J Photochem Photobiol A Chem 164:3
2. Murakami T, Graetzel M (2008) Inorg Chim Acta 361:572

3. Koo BK, Lee DY, Kim HJ, Song JS, Kim HJ (2006) J Electroceram 17:79
4. Fang X, Ma T, Guan G, Akiyama M, Kida T, Abe E (2004) J Electroanal Chem 570:257
5. Kern R, Sastrawan R, Ferber J, Stangl R, Luther J (2002) Electrochem Acta 47:4213
6. Sakaguchi S, Ueki H, Kato T, Kado T, Shiratuchi R, Takashima W, Kaneto K, Hayase S (2004) J Photochem Photobiol A Chem 164:3117
7. Murai S, Mikoshiba S, Sumino H, Hayase S (2002) J Photochem Photobiol A Chem 148:33
8. Wilburn DR, Bleiwas DI (2004) Platinum-group metals-world supply and demand. US geological survey open-file report
9. Kay A, Gratzel M (1996) Sol Energy Mater Sol Cells 44:99
10. Wroblowa HS, Saunders A (1993) Electroanal Chem Int Electrochem Soc 115:6382
11. Tarasevich MR, Khrushcheva EI (1989) In: Conway BE, Bockris J, White RE (eds) Modern aspects of electrochemistry, vol 19. Plenum Press, New York
12. Ramasamy E, Lee WY, Song JS (2007) Appl Phys Lett 90:173103
13. Murakamy A, Ito TNS, Wang Q, Nazeeruddin MK, Bessho T, Cesar I, Liska P, Baker RH, Comte P, Pechy P, Graetzel M (2007) J Electrochem Soc 153:A2255
14. Hino T, Ogawa Y, Kuramoto N (2006) Carbon 44:880
15. Huang Z, Liu X, Li K, Luo Y, Li H, Song W, Chen L, Meng Q (2007) Electrochem Commun 9:596
16. Imoto K, Takahashi K, Yamaguchi T, Komura T, Nakamura J, Murata K (2003) Sol Energy Mater Sol Cells 79:459
17. Lee WI, Ramasamy E, Lee DY, Song JS (2008) J Photochem Photobiol A Chem 194:27
18. Lee WI, Ramasamy E, Lee DY, Song JS (2008) Sol Energy Mater Sol Cells 92:814
19. Hauch A, Georg A (2001) Electrochim Acta 46:3457
20. Kinoshita K (1988) Carbon, electrochemical and physicochemical properties. Wiley-Interscience Publication, New York
21. Medalia AI, Rivin D (1976) In: Parfitt GD, Sing KSW (eds) Characterization of powder surfaces. Academic Press, London
22. Boukamp BA (1986) Solid State Ionics 29:31
23. Sakane H, Mitsui T, Tanida H, Watanabe I (2001) J Synchrotron Radiat 8:674
24. Wang Q, Moser J, Graetzel M (2005) J Phys Chem B 109:14945
25. Van de Lagemaat J, Park NG, Frank AJ (2000) J Phys Chem B 104:2044
26. Aricò AS, Antonucci V, Minutoli M, Giordano N (1989) Carbon 27:337